Evaluation of Ti Aluminide Intermetallics Processed Through Reaction Synthesis

R. K. Gupta*,[1], Bhanu Pant[1], Vijaya Agarwala[2], R. C. Agarwala[2] and P. P. Sinha[1]

[3] *Vikram Sarabhai Space Centre, ISRO, Trivandrum – 695 022*
[2] *Indian Institute of Technology, Roorkee, Roorkee – 247 667*

(Received January 7, 2009

ABSTRACT

Titanium aluminides based on Ti48Al with Cr and Nb additions has been made through reaction synthesis (RS) process. Development of various phases in RS and after homogenization has been studied through X-ray diffraction (XRD), optical microscopy (OM) and Transmission Electron Microscopy (TEM). Uniform distribution of elements was confirmed through elemental mapping, EDAX and hardness measurements. It is observed that, mainly Al_3Ti phase forms during reaction synthesis and TiAl (γ) and Ti_3Al (α_2) phases form after homogenization. Density of the product was measured and found to be nearly equal to theoretical density of the alloy. Improvement in hardness is observed after homogenization, which is found to be due to formation of γ. phases. A high temperature oxidation study of the ternary and quaternary alloy was carried out and it was noted that oxidation resistance of quaternary alloy is better than ternary alloy (with Cr). Processing aspects and properties of present alloys is compared with RS processed binary Ti alumnide.

1. INTRODUCTION

Ti aluminide has been an important aerospace material due to its high temperature properties and lower density as compared to superalloys. Most useful gamma titanium aluminides are centered around Ti-46-52at%Al composition which belongs to the γ (TiAl) plus α_2 ($T_{i3}Al$) region of the phase diagram /1/. These aluminides can be tailored to have a variety of microstructures by heat treatment and by alloying additions, resulting in the desired properties. Several workers have studied this class of aluminides employing different processes /2-19/. In the recent years, studies have been focusing through self propagating high temperature synthesis (SHS) process also known as reaction synthesis process of powder metallurgy route /20-29/, where heat of reaction is utilized in synthesis of aluminide. It has the advantage of uniform distribution of elements resulting in uniformity of stiochiometric composition in the alloy.

Alloying addition of Cr to two-phase titanium aluminides containing γ and α_2 phases enhances the ductility whereas Nb additions improve strength and oxidation resistance /30/. Both of these alloying elements have excellent solubility in both the γ and α_2 phases. However, Nb has more solubility in the two phases and forms no intermetallic phases both with Ti and Al in small concentrations /31/. Further, it is reported that alloying addition of Nb enhances diffusivity of Ti in TiAl /32/ due to elastic distortion of the L10 structure caused by oversized Nb atoms. The atomic sizes of Ti, Al, Cr and Nb are reported in literature as 0.24861, 0.13607, 0.22701 and 0.32071 nm, respectively /33/. High solubility and good diffusivity of

* Corresponding Author: Ph.: +91-471-2562484, Fax: +91-471-2705427
E-mail: rohitkumar_gupta@vssc.gov.in

Cr and Nb in γ and α_2 phases make them suitable for alloying additions and render the ternary and quaternary alloys amenable to reaction synthesis (RS). Studies on RS of binary γ-TiAl have been reported /22, 34-38/ but studies on quaternary alloys are limited /39, 40/. Some studies on RS of the important ternary alloy Ti-Al-Cr and quaternary alloy Ti-Al-Cr-Nb alloys have been made /41/ and further it is presented here.

In this work, two important alloys are studied namely ternary Ti-48Al-2Cr (at%) and quaternary Ti-48Al-2Cr-2Nb (at%). Reaction synthesized and homogenized alloy was characterized through X-ray diffraction (XRD), Optical microscopy (OM), Electron diffraction analysis through X-ray (EDAX), elemental mapping, Transmission Electron Microscopy (TEM), Vickers hardness and density measurement. Also, uniformity of the large 75 mm diameter billets is investigated with respect to phases present, and microstructure across the section of the billet. Oxidation behaviour of the ternary and quaternary samples has also been studied. Finally the alloy processing and properties are compared with RS processed binary alloy /38/.

2. EXPERIMENTAL

Firstly, smaller compacts of 30 mm diameter were hot pressed under argon then larger diameter billets (75 mm) were made in vacuum hot press. The experiments have been carried out at a temperature of 1073K with applied pressures of 111 MPa.

2.1 Raw material

Titanium powder (99.5% purity, 16 μm average particle size) of Merck, Aluminum powder (99.0% purity, 24 μm average particle size) of Metal Powder Company Madurai, Chromium powder (99.5% purity, -100 mesh average particle size) of Aldrich and Nb powder (99.8% purity, -325 mesh average particle size) of Acros Organics were used in the experiments. The morphology of titanium, aluminum, chromium and niobium powders taken through LEIKA S440i make scanning electron microscope is presented in Fig. 1.

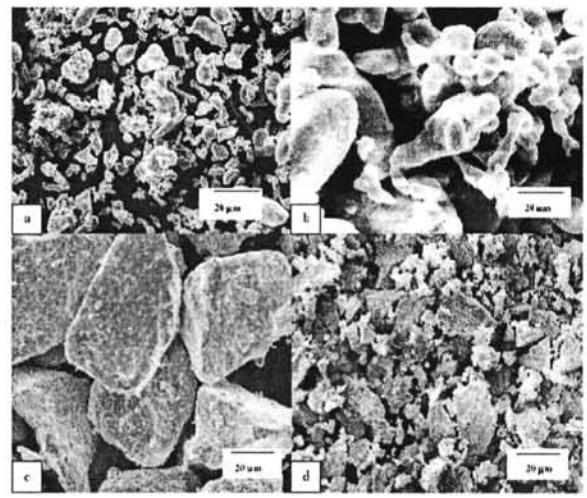

Fig. 1: SEM photomicrographs of the elemental powders of (a) Ti, (b) Al, (c) Cr and (d) Nb

2.2 Preparation of powder mix

The elemental powders were weighed using Sartorius Austria make precision balance and mixed in a Fritsch, Germany make P5 Planetary ball mill. Agate jars and spherical balls were used for blending. Three cycles of 45 min running + 10 min pause at 100 rpm was used with suitable ratio of balls to charge. For the smaller diameter (30 mm) pellets, a blended charge of about 55g was cold pressed by applying 5 tons load and for bigger diameter (75 mm) billets 1.1 kg blended charge was cold pressed by applying 20 tons load. For both the experiments, dies and punches made of Inconel 718 material were used and zinc stearate was used as lubricant. After the cold pressing, compacts of approximately 60% density were obtained.

2.3 Reaction synthesis

Smaller diameter pellets (30 mm dia.) were hot pressed at 1073K with 111MPa pressure under argon. Inconel 718 material die and punch were used and Fluka make fine graphite powder was used as lubricant. Soaking of 1 hour was given at 1073K. For billets (75 mm dia.) also Inconel 718 material die and punch was used and fine boron nitride powder was used as lubricant. Hot pressing was carried out at 1073K with 111MPa pressure in vacuum. Soaking of 1 hour was

given at 1073K maintaining pressure and then the furnace was switched off and the load was released. Hot pressed pellets/ billets were carefully removed by pressing in reverse direction using smaller punch in another hydraulic press. Reaction synthesized pellets and billets were designated as TACp and TACb for ternary alloy and TACNp and TACNb for quaternary alloy respectively.

2.4 Homogenising treatment

Homogenising treatment of various hot pressed pellets and billets was carried out at temperature of 1523K i.e. in the two-phase ($\alpha+\gamma$) field where α and γ phases are approximately in equal proportion. Vacuum heat treatment furnace with Molybdenum heating elements was used for this treatment. Homogenising times of 4 hours were imparted according to studies made on binary alloy /38/.

2.5 Characterisation

The density of reaction synthesized and homogenized samples was measured following Archimedes principle and using density measurement kit available with Sartorius balance.

For X-ray diffraction analysis, the solid sample of approximate size 25 mm dia was used. XRD observations were made in a 75 mm dia billet at various points (Fig. 2). Phillips X-ray diffractometer (model PW1140/90) was used in the angle range of 5-100°, with Cu Kα (λ=0.15405 nm) target and with goniometer speed of 0.01°/m. The interplaner spacing for various phases was calculated from their corresponding 2θ values using Bragg's Law and different phases were identified through JCPDS files.

Elemental mapping and EDAX analysis was done to study distribution and content of various elements using scanning electron microscope of Leo model number 440i with accelerating voltage of 20 kV.

Optical metallography specimens were prepared using conventional polishing technique and Kroll's reagent was used for etching. The optical microscope of Leico make was used for observation. Transmission electron microscopy of selected samples was carried out using Phillips CM12 model at 120kV. TEM specimens were prepared through electrolytic thinning. The electrolyte of 6% H_2SO_4 and 94% methanol cooled in liquid nitrogen was used in electrolytic thinning. TEM micrographs were taken along with the selected area diffraction (SAD) pattern. The d values were calculated and matched with the JCPDS files to identify various phases. Further, the phases were confirmed by calculating the angle between two planes and by actual measurement on the SAD pattern.

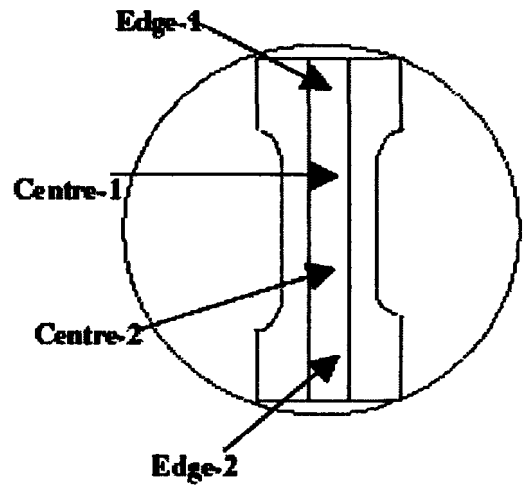

Fig. 2: Schematic diagram showing tensile specimen cutting location and observation points for hardness, XRD and microstructure evaluation of 75 mm diameter billet

The homogeneity of 75 mm diameter billet was verified by taking measurements of Vickers hardness and XRD across the section at locations shown schematically in Fig. 2. Vickers's hardness measurement was carried out at 20Kg load using Blue Star make hardness tester.

2.6 Oxidation studies

Samples of size approximately 7X5X4 mm were prepared using an EDM sawing machine and polished using a precision surface grinder with a fine silicon carbide wheel. A tubular furnace of Heraus make was used and samples were suspended into furnace using platinum wire. Weight and dimensions of each sample

were measured before the oxidation studies using five digit precision balance from Sartorius. Various samples were exposed to a temperature of 973 K for varying times up to 7200 s and the weight gain with time was recorded.

3. RESULTS AND DISCUSSIONS

3.1 Density measurements

The density levels achieved for both ternary and quaternary alloys are presented in Table 1. Near full density is achieved for all the samples as the reaction synthesis was carried out under high temperature and pressure /38/. From Table 1 it is seen that density variation is much less for both ternary and quaternary samples and 98.6 to 100% relative density has been achieved. This is due to the same level of pressure (111 MPa) applied during RS for ternary and quaternary samples. In the case of binary alloy also /38/ this level of density was reported, indicating that ternary and quaternary alloying additions (Cr and Nb) do not have a significant effect on densification and it is mainly governed by process parameters (pressure and temperature).

Table 1

Density achieved for ternary and quaternary samples at RS pressure of 111 MPa

Sl. No.	Sample No.	Density Achieved 10^{-6} x gm/m^3	Composition	% of theoretical density
1	TACp	3.79	Ti-48Al-2Cr	99.7
2	TACb	3.80	Ti-48Al-2Cr	100
3	TACNp	3.75	Ti-48Al-2Cr-2Nb	98.6
4	TAC Nb	3.80	Ti-48Al-2Cr-2Nb	100

3.2 Optical metallography

Optical microstructures of ternary as-pressed and homogenized samples are shown in Fig. 3. It is observed that as pressed microstructure (Fig. 3a) contains bright Ti-rich and dark Al-rich regions with various shades of gray contrast indicating that darker the shade, the higher is the Al content of the phase. The bright phase is Ti-rich phase, where minimum diffusion of Al has occurred. An intermediate phase is seen to be present at the interface of Ti-rich and Al-rich regions. The optical microstructures of the ternary homogenized sample (Fig. 3b) show duplex-type structure where lamellar ($\gamma + \alpha_2$) phases are formed by the nucleation and growth from high temperature α phase /38/. Content of lamellar phase is relatively higher than the binary alloy processed with the same parameter /38/. Lamellar phase formation in Ti aluminide is promoted by Cr /5, 42/. This is attributed to the availability of more alpha phase at homogenization temperature of 1523 K, since Cr addition tends to suppress both the γ-solvus as well as α-transus /5/. The optical microstructure of the as-pressed quaternary alloy samples was similar to ternary alloy except for the intermediate region for quaternary alloy, which is formed to a relatively larger width. This is attributed to higher diffusivity of Ti /32/ in case of quaternary alloy as compared to ternary alloy owing to the presence of large Nb atoms in the lattice in the quaternary samples. It is explained in detail /41/. The optical micrographs of samples taken from locations near the edges and from the central portions of the 75 mm diameter billets did not show any variation in the microstructure.

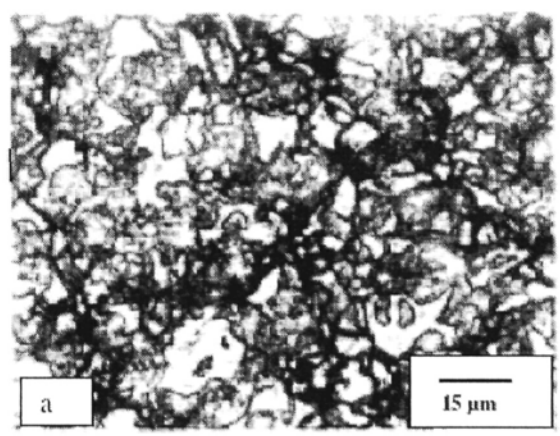

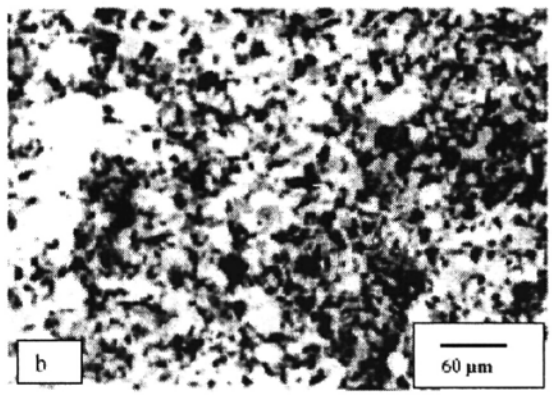

Fig. 3: Optical micrographs of TAC alloy (a) as pressed (b) homogenized sample

3.3 SEM Elemental mapping and EDAX point analysis

The SEM elemental mapping results for the elements Al and Ti for as-pressed samples of ternary and quaternary alloy were similar. A representative map of TACNb samples is presented in Fig. 4. Distinct regions of Ti-rich and Al-rich phases are observed. However, in the case of homogenized samples, better homogeneity was observed in quaternary alloy as compared to ternary alloy. The elemental mapping of $TACN_b$ homogenized sample is presented in Fig. 5. Homogenized sample of $TACN_b$ (TACNb-H) exhibits more homogeneous elemental distribution. Better elemental homogeneity is attributed to Nb addition effect in quaternary alloy /32/.

To verify actual elemental concentration at various regions, EDAX point analysis is carried out at four points as shown in Figs. 4-5 and the results are presented in Table 2. The points 1 and 2 represent maximum Ti and Al locations of as-pressed samples whereas 3 and 4 points describe possible composition variation in the homogenized samples. As seen from Table 2, the as-pressed sample shows non-homogeneity whereas the homogenized sample has quite uniform Ti, Al, Cr and Nb content. However, minor variation in Ti and Al content is noted after homogenization. This may be due to a small variation in the elemental content within the sample. A relatively lower Ti region (darker) within the band of 47-52 Ti (at%) results in γ-phase as the presence of more Al in these regions stabilizes γ-phase and other regions correspond to duplex structure.

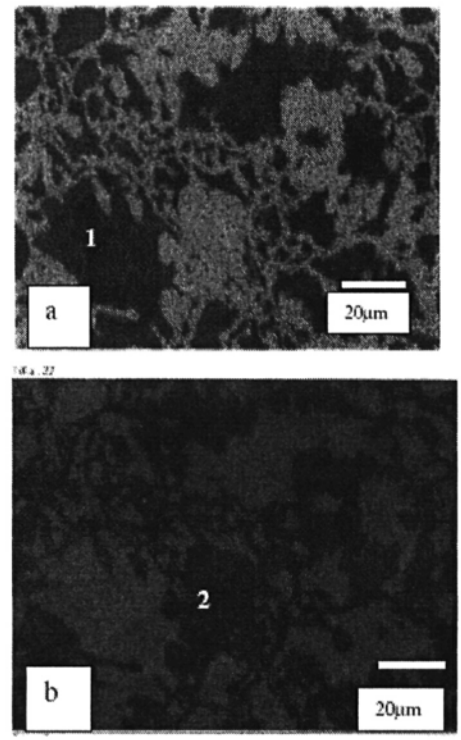

Fig. 4: Representative SEM elemental mapping of as-pressed sample showing distribution of: (a) Ti and (b) Al in TACN

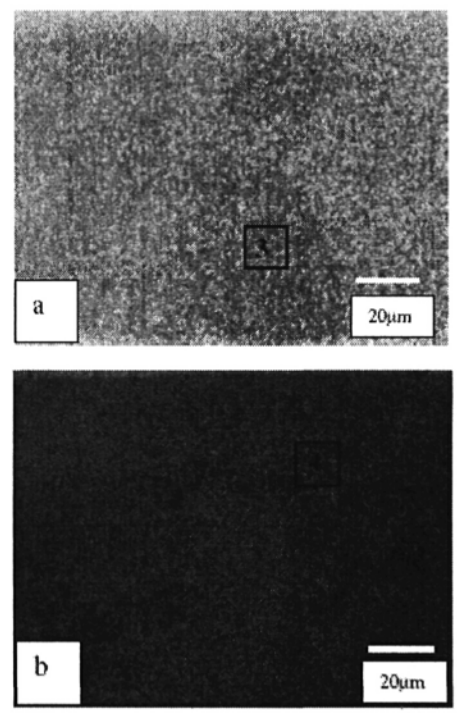

Fig. 5: Representative SEM elemental mapping of homogenised sample showing distribution of: (a) Ti and (b) Al in TACN

Table 2
Results of EDAX analysis for as-pressed and homogenised TACN samples

Location	Content (at. %)				Sample Condition
	Al	Cr	Nb	Ti	
1 (Fig. 4)	3.4	0.5	0.6	95.1	TACN (As-pressed)
2 (Fig. 4)	70.5	1.2	1.1	29.5	TACN (As-pressed)
3 (Fig. 5)	47.2	0.88	0.86	51.06	TACN (Homogenised)
4 (Fig. 5)	49.7	1.1	1.05	48.2	TACN (Homogenised)

3.4 X-Ray Diffraction (XRD)

In the as-pressed samples of both TAC and TACN alloys Al3Ti, TiAl with Ti elemental phase was detected. In this respect, the Al3Ti phase formation occurs in the as-pressed condition similar to binary alloy samples /38/. However, the homogenized treatment of four hours at 1532K results in stable TiAl plus Ti_3Al phases in both the alloys. Additionally, presence of Cr and Nb enhances the diffusivity of elements in intermetallic phases and therefore reduce the time required to achieve homogenisation. The phase formation sequences are similar to binary alloy processed with similar parameters and is described in detail elsewhere /38, 41/. A typical XRD plots for homogenised TACNb sample is presented in Fig. 6.

3.5 Transmission Electron Microscopy (TEM)

The TEM micrographs from two regions of the as-pressed TAC sample and corresponding SAD patterns are presented in Figs. 7 and 8. The phases in the as–pressed samples are observed to be Al_3Ti, Ti (Fig. 7) and Ti_3Al (Fig. 8). However, the XRD results for this sample have not shown any Ti_3Al, implying the content of this phase is very small. Twinned spots are observed in the SAD pattern shown in Fig. 8 corresponding to Ti_3Al ($\alpha 2$) phase. The applied pressure during RS causes the formation of deformation twins. Deformation twins occur commonly in hcp crystals /43/ and so in α_2 phase being ordered hcp type DO_{19} crystal structure.

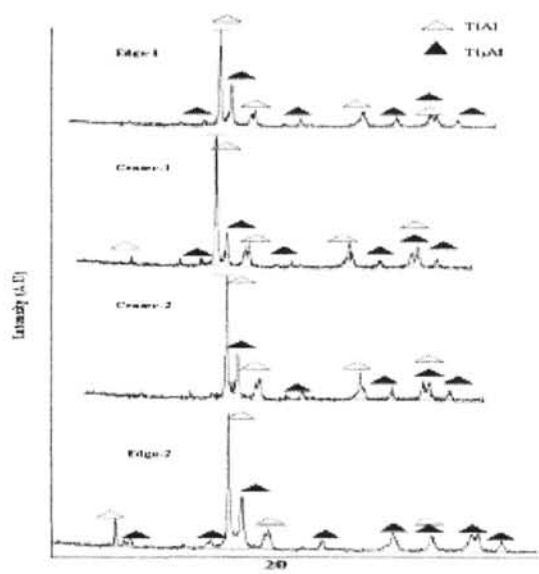

Fig. 6: Typical XRD plots through section of 75 mm diameter TACN-H sample

The TEM micrograph of the homogenized TAC sample (TAC-H) from lamellar γ plus α_2 region is shown in Fig. 9. The phase relationship γ/α_2 in the lamellar structure is found to be [011]/ [010]. The width

of γ lamellae in the ternary TAC alloy is found to be about 125 nm whereas α_2 lamellae have a width of about 60 nm as measured from Fig. 9. In comparison, the α_2 lamellae width for binary sample is measured to be 150 nm whereas the width of α lamellae is about 180 nm /38/. Thus, it is observed that lamellar width for ternary sample is finer as compared to the binary sample. This lamellar structural refinement is attributed to lowering of the α to lamellar transformation temperature due to Cr addition /5/.

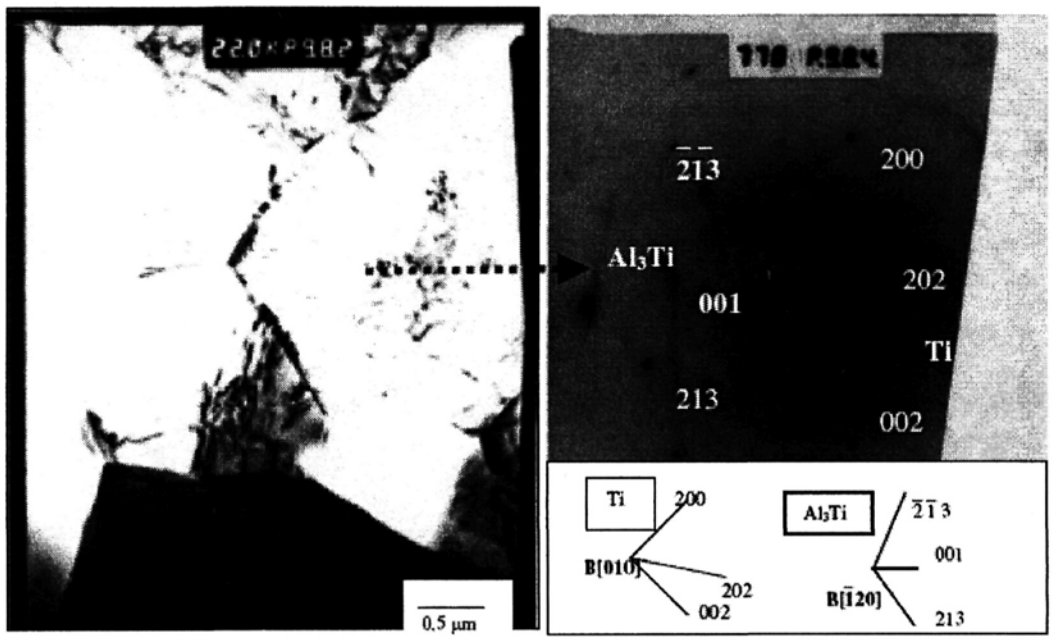

Fig. 7: TEM micrograph and SAD pattern of as-pressed TAC sample from a region showing Ti and Al_3Ti phases

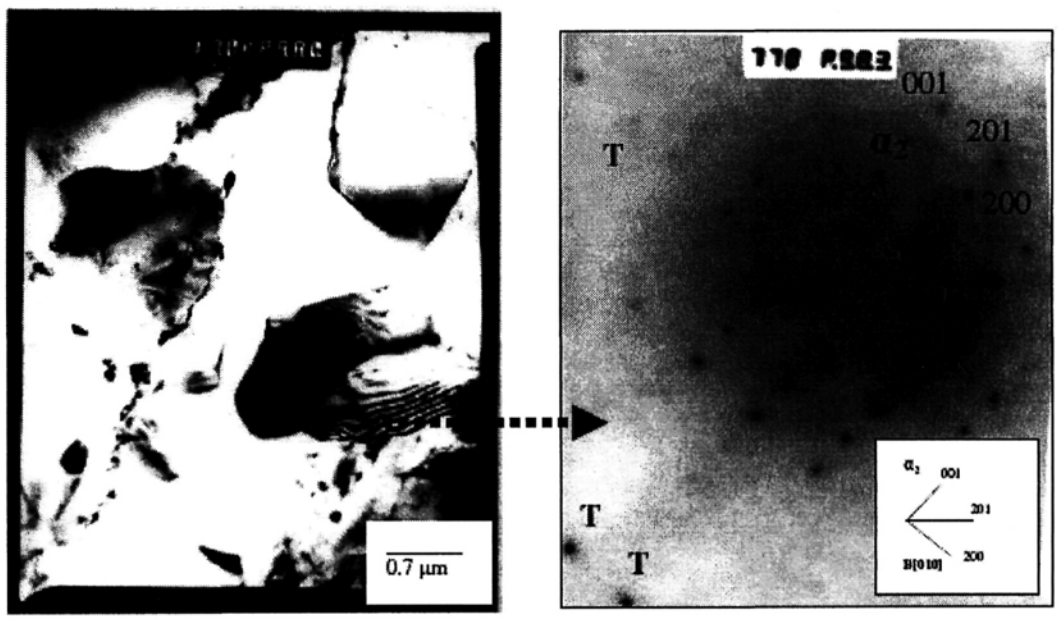

Fig. 8: TEM micrograph and SAD pattern of as-pressed TAC sample from a region showing □2 phase with twinned spots 'T'

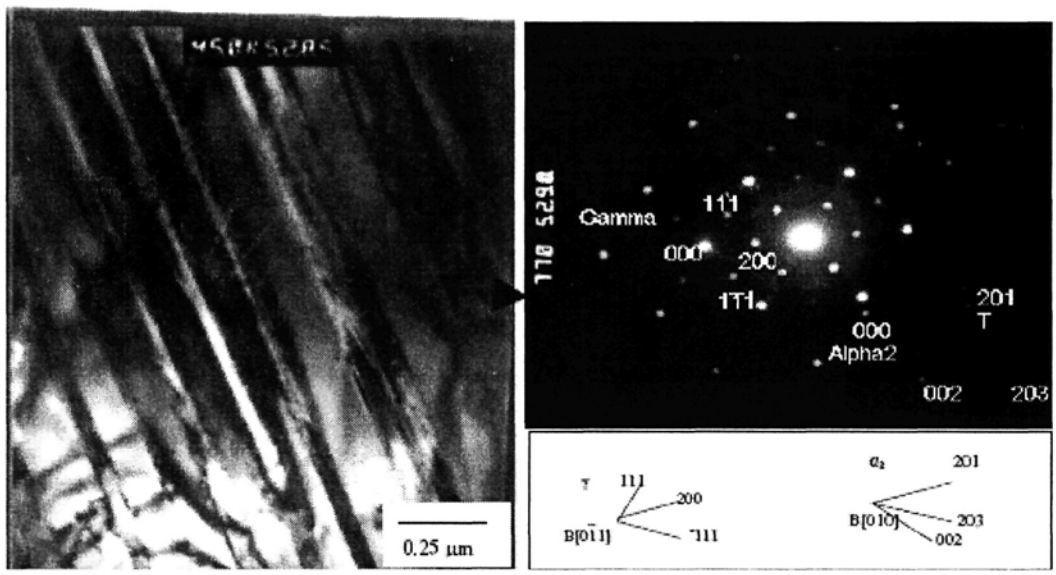

Fig. 9: TEM micrograph of TAC-H sample showing lamellar region and corresponding SAD pattern

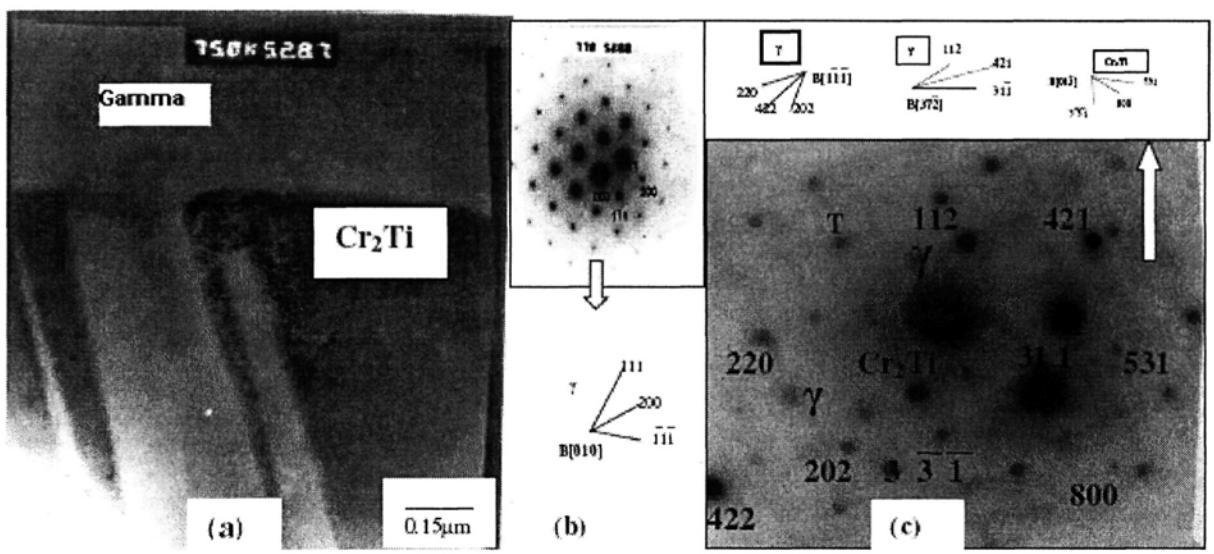

Fig. 10: (a) TEM micrograph of TAC-H sample showing γ and Cr_2Ti regions, (b) SAD pattern at γ region of (a) and (c) SAD Pattern at Cr_2Ti region of (a)

The TEM of the TAC homogenised sample is carried out at a region where three phases are observed in the sample and the same is presented in Fig. 10. The SAD patterns obtained from the two locations are marked in the TEM micrograph as gamma and Cr_2Ti. The ternary Ti-Al-Cr isotherm at 1273 K shows formation of Cr_2Ti at about 60 at% Cr /31/. Thus, the presence of Cr_2Ti phase in Fig. 10 indicates some amount of segregation for element Cr at the grain boundary. However, Cr_2Ti peaks are not present in the XRD plot of this sample indicating the content of this phase may be small. The width of Al-rich darker region (γ) is found to be increased in the region adjacent to the Cr2Ti phase due to Ti depletion in the region.

TEM of the TAC homogenized sample is shown in Fig. 11 where lamellar structure growing from the gamma grain boundary is observed. The SAD pattern however, is from the lamellar region and found to contain α_2 and γ phases. Twinned spots are also observed which are deformation twins formed in hcp

DO19 type Ti3Al phase. The source of twins may be the stress applied during RS process as reported by Hemker et al. /44/.

TEM of quaternary samples also showed the same phases as seen in ternary alloys in the as pressed and homogenized condition.

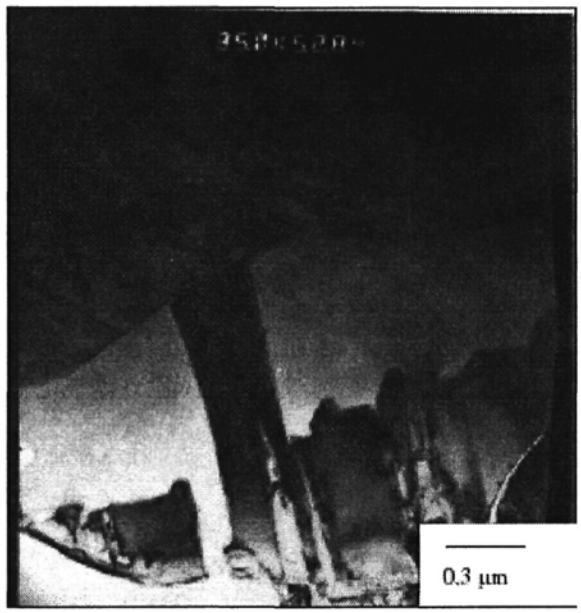

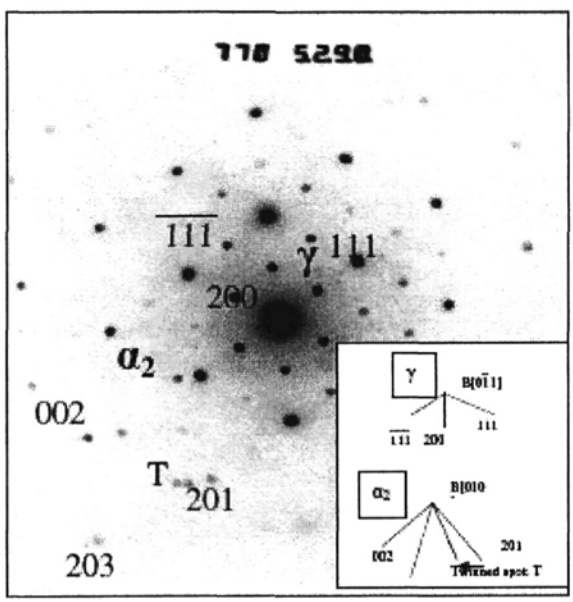

Fig. 11: TEM micrograph of TAC-H sample with SAD pattern for lamellar region with twinned spot

3.6 Homogeneity analysis of 75 mm diameter billets

After completing the RS experiment on 30 mm diameter samples, larger billets of 75 mm diameter are processed. This study is carried out to ascertain the homogeneity of larger samples as the cross section has increased by 6.25 times. Hence, XRD measurement of samples cut from various regions of the 75 mm diameter billet and measurement of hardness across the section was carried out. The XRD from different locations were studied and the uniformity of phases present in the billet at various locations is confirmed. The samples contain stable TiAl and Ti_3Al phases after homogenization.

Vickers hardness across the section of homogenized ternary and homogenized quaternary billets was measured to evaluate the variation. The hardness measurement results are presented in Fig. 12. Hardness measurement points were marked at an interval of 7 mm starting from one edge of 11 the billet. It is observed that, Vickers hardness varies from 274 to 303 for the ternary homogenised billet. The variation of hardness is found to be in quite a narrow band.

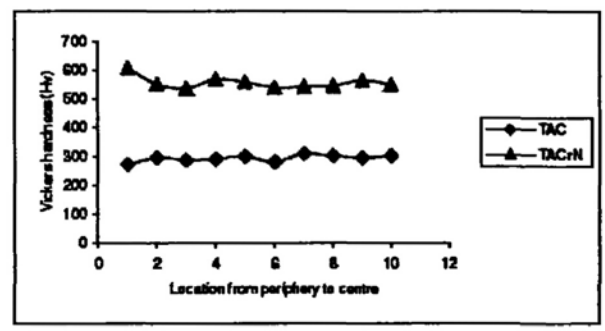

Fig. 12: Variation of Vickers hardness across diameter of billet

The variation is observed to be in slightly broader range from 542 to 610 Hv for homogenized quaternary billet. This variation is related to the presence of some softer γ phase rich regions in the billet. The higher hardness in the quaternary alloy is derived from the presence of large amount of lamellar phase /45, 46/ as compared to ternary alloy where content of γ phase rich regions is found to be greater. This is in line with the report that Cr favours γ phase and Nb favours lamellar phase formation /3/. Improvement in hardness due to Nb

addition is also reported by Dulal and Ghosh /30/.

3.7 High temperature oxidation studies

The weight gain per unit area was calculated for various conditions (see Table 3) and is shown in Fig. 13. It is seen from this figure that Cr containing TAC homogenized (TAC-H) sample has minimum oxidation resistance (as seen from the rate of increase of weight-gain per unit area) as compared to binary TiAl /38/ and $TACN_b$ homogenised ($TACN_b$-H) samples. It is reported in literature that Cr additions of less than 4 at.% have a detrimental effect but dramatically improve oxidation resistance above 8 at% /47, 48/. At 2 at% Cr, formation of TiO_2 is preferred as compared to Al_2O_3 and hence the oxidation resistance of the TAC alloy is the least. It is seen in the present work that in the ternary Cr containing samples, Cr tends to segregate at the grain boundaries as shown by TEM micrograph in Fig. 10 and this grain boundary segregation of Cr can lead to higher oxidation in the Cr containing samples.

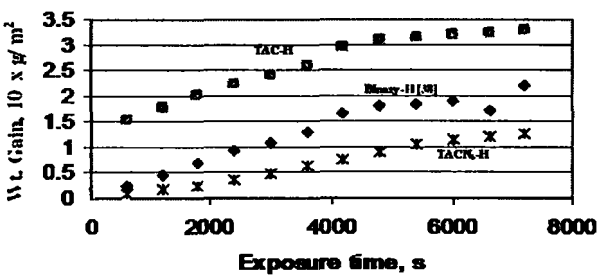

Fig. 13: Comparison of weight gain per unit area for binary, ternary and quaternary samples

Table 3

Weight gain per unit area for various ternary and quaternary samples after exposure to 973K for 7200s

Sl. No.	Sample Id.	Weight gain/ unit area, g/m^2
1	TAC-H (Homogenised)	33.0
2	TACN (As-pressed)	13.1
3	TACN (Homogenised)	12.5

The oxidation resistance of TACN homogenised samples (TACN-H) is observed to be the best. It is reported that additions of Nb to titanium aluminides improve the oxidation resistance by improving diffusivity of Al in the Nb-stabilised β phase /47, 49/. This enhanced diffusivity of Al enables the formation of protective Al_2O_3 layer which is adherent /48/ on the surface thereby improving the oxidation resistance of the sample. Comparing the slopes of the plots in Fig. 13 for various samples, it is seen that the comparable slopes or rates of oxidation are observed for binary and ternary samples whereas the slope for the quaternary sample is smaller by an order of magnitude. The small slope or slower oxidation rate is attributed to the oxidation behaviour improvement by Nb additions in the quaternary samples. The flattening of the plot occurs at an early stage for binary and ternary sample while the onset of the plateau for quaternary sample is observed at a later stage. This is attributed to the slower oxide layer thickness build up that protects the sample in the quaternary alloy samples as compared to the binary and ternary samples.

4. CONCLUSIONS

Full density products of ternary Ti48Al2Cr and quaternary Ti48Al2Cr2Nb alloys have been obtained using RS technique. The as-pressed samples are non-homogenous and contain Al_3Ti as the major phase along with Ti. These samples are homogenized by heat treatment at 1523 K for 4 hours. Stable phases like TiAl and Ti_3Al are observed in the homogenized samples which show γ and α_2 phases and exhibit microstructures consisting of lamellar (γ plus α_2) and γ grains for both the ternary and quaternary alloys. The RS studies results for ternary and quaternary alloys are compared with binary alloys. In the ternary and quaternary alloys no remnant Al is observed due to better diffusivity of Al resulting in complete reaction in these alloys.

Average Vickers hardness values for ternary Ti48Al2Cr and quaternary Ti48Al2Cr2Nb alloys produced by RS are found to be 295 and 559 respectively. Oxidation studies show that best oxidation resistance is achieved for quaternary Cr-Nb containing alloy whereas ternary Cr containing alloy has the worst oxidation resistance The poor oxidation resistance of ternary aluminides may be related to the Cr_2Ti phase

formation at the grain boundaries. Improvement of alumina-forming tendency in quaternary Nb containing alloy may be due to better diffusivity of Al that leads to superior oxidation resistance in these alloys.

ACKNOWLEDGEMENTS

The authors are thankful to Head SMF and Head MCD of VSSC and Head, IIC, IIT Roorkee for hot pressing and characterization facility support. The authors extend their thanks to Director, VSSC for permission to publish this work.

REFERENCES

1. U. R. Kattener, J. C. Lin and Y. A. Chang, *Met Trans A,* **23A**, 2081(1992).
2. H. A. Lipsitt, *High Temp Ordered Intermetallic Alloys,* Eds C. C. Koch, C. T. Liu and N. S. Stolloff, MRS, 39 (1985) 351-364.
3. M. Lamirand, J.L. Bonnentien, G. Ferriere, S. Guerin and J.P. Chevalier, *Scripta Mater.*, **56,** 325 (2007).
4. T. Toshimitsu, *Mater Sci Eng,* **A329-331,** 582 (2002).
5. S. C. Huang and E. L. Hall, *High Temp Ordered Intermetallic Alloys IV,* Eds L. A. Johnson, D. P. Pope and J. O. Stiegler, *Mater Res Soc Symp Proc,* **213**, (1991) 827-832.
6. T. Tetsui, *Intermetallics,* **10,** 239–245 (2002).
7. M. Yamaguchi, *Mater Sci Tech,* **8,** 299 (1992).
8. M. Yamaguchi, H. Inui and K. Ito, *Acta Mater,* **48,** 307-322 (2000).
9. D. K. Peacock, *Met Mater,* **5,** 474 (1989).
10. B. Bondarev, N. Anoshkin, A. Molotkov, A. Notkin and D. Elagin, *Intermetallic Compounds-Structure and Properties,* Eds O. Izumi, The Japan Inst of Metals, Sendai, (1991) 1009.
11. R. M. Imayev, V. M. Imayev and G. Salischev, *Scripta Mater,* **29,** 713-718 (1993).
12. R. M. Imayev, V. M. Imayev and G. Salischev, *Scripta Mater,* **29,** 719-724 (1993).
13. G. Salischev, R M. Imayev, O. N. Senkov and F. H. Froes, *JOM,* 46-48 (2000).
14. G. Salischev, R M. Imayev, O. N. Senkov, V. M. Imayev, N. K. Gabdullin, M. R. Shagiev, A.V. Kuznestov and F. H. Froes, *Mater Sci Eng,* **A286,** 236-243 (2000).
15. M.R. Shagiev, G. Salischev, R. M. Imayev, V. M. Imayev and A. V. Kuznestov, *Mater SciForum,* **447-448**, 317-322 (2004).
16. J. Baczewska Karwan, T. Dymkoski and S. Seetharaman, *Adv in P M and Particulate Mater,***4** (15), 15-3 (1996).
17. G. Sauthoff, *Intermetallics,VCH Verlags-gesellschaft mbH,* Germany (1995) 1-16.
18. B. Dogan, R. Wagner and P. A. Beaven, *Scripta Met,* **25,** 773-778 (1991).
19. M. Dahms, J. Seeger, W. Smarsly and B. Wildhagen, *ISIJ Int,* **31,** 1093-1099 (1991).
20. A. P. Savstkii, *Soviet P M Metal Ceramics,* **19,** 488 (1980).
21. A. P. Savstkii and N. N. Brutsev, *Soviet P M Metal Ceramics,* **20,** 681-621 (1981).
22. N. Bertolino, M. Monagheddu, A. Tacca, P. Giuliani, C. Zanotti and U. Tamburini Anselmi, *Intermetallics,* **11,** 41 –49 (2003).
23. D. J. Lee and D. N. Yoon, *P M Int.,* **20,** 15 (1988).
24. A. Bose, B. H. Rabin and R. M. German, *P M Int.,* **20,** 25 (1988).
25. C. Nishimura and C. T. Liu, *Acta Mater,* **41,** 113-120 (1993).
26. J. T. Guo and C. Y. Cui, *Key Eng Mater,* **217,** 117-128 (2002).
27. G. Zhenbin, K. Chen, J. Guo, H. Zhou and J. M. F. Ferreira, *J European Ceramic Soc,* **23,** 567 –574 (2003).
28. B. H. Rabin and R. N. Wright, *Met Trans A,* **22A,** 277 (1991).
29. S. Gedevanishvili and S. C. Deevi, *Mater Sci and Eng,* **A325,** 163-176 (2002).
30. Y. W. Kim and F. H. Froes, *High Temp Aluminides and Intermetallics,* Eds S. H. Whang, C.T. Liu, D. P. Pope, (1990) 465-492.
31. M. Palm and G. Inden, *Structural Intermetallics,* Eds M.V. Nathal, R. Darolia, C. T. Liu, P. L. Martin, D. B. Miracle, R. Wagner and M. Yamaguchi, The Minerals, Metals and Mater

Society, (1997) 73-82.

32. J. Breur, T. Wilger, M. Friesel and C. Herzig, *Intermetallics,* **7,** 381 (1999).
33. C. Dulal Ghosh and R. Biswas, *Int J Mat Sci* , 3, 87-113 (2002).
34. Wu Yinjiang, Zhang Xiaoming, Li Ying Guan, Yin Weihong, Zhon lian , Jin Zhihao, *Key Engg Mater,* **217,** 111-116 (2002).
35. Qian Wang, Zhengming Sun, Hitoshi Hashimoto, Shuji tada, Yong-ho Park, Se-Hyun Ko and Toshiko Abe, *Mater Trans JIM,* **41** (5), 551-554 (2000).
36. C. E. Wen, K. Yasue and Y. Yamada, *J Mater Sci,* **36,** 1741-1745 (2001).
37. J. C. Rawers and W. R. Wrzesinky, *J Mater Sci* , **27,** 2877-2886 (1992).
38. R. K. Gupta, B. Pant, V. Agarwala, R.C. Agarwala and P.P. Sinha, *J. Mater. Sci. Techno.* – in press.
39. B.J. Lee and N. Saunders, *Z. Met,* **88,** 152-161 (1997).
40. T. K. Lee, E. I. Mosunov and S. K. Hwang, *Mater Sci Eng,* **A239-240,** 540-545 (1997).
41. J. K. Kim, T. K. Kin, T. K. Lee, S. K. Hwang, S. W. Nam and N. J. Kim, *Gamma Ti Aluminides,* Eds Y. W. Kim, D. M. Dimiduk and M. H.Loretto, The Minerals, Metals and Material Society, (1999) 231-238.
42. B. Pant, V. Agarwala, R.C. Agarwala and P.P. Sinha, *Trans. Ind. Inst. of Metals,* **60** (4), 407-416 (2007).
43. Y. W. Kim *JOM,* **46** (7), 39-41 (1995).
44. K. J. Hemker, M. Lu and M. Zupan, *Structural Intermetallics*, Eds M. V. Nathal, R. Darolia, C. T. Liu P. L. Martin, D. B. Miracle, R. Wagner and M. Yamaguchi, The Minerals, Metals and Mater Society, (1997) 147-156.
45. G. X. Wang and M. Dahms, *Scripta Mater,* **26,** 717-722 (1992).
46. S. Hamada, H. Hamada H., Suzuki and A. J. Nozue, *J Mater Sci,* **37,** 1107-1113 (2002).
47. S. C. Huang and J. C. Chesnutt, *Intermetallic Compounds,* Eds J. H. Westbrook and R. L. Fleisher, John Wiley and Sons, 2, (1994) 73 – 90.
48. Yang Mu-Rong and Wu Shyi-Kaan, *Bulletin of the College of Eng, N.T.U., 89, 3*–19 (2003)
49. J. Doychak, *Intermetallic Compounds*, Eds J. H. Westbrook and R. L. Fleischer John Wiley and Sons, 1, (1994) 977-1016.